Optics & Laser Technology 156 (2022) 108576

Contents lists available at ScienceDirect

Optics and Laser Technology

journal homepage: www.elsevier.com/locate/optlastec

Research Note

Study of crystalline growth, structural characteristics, optical behavior, thermo and dielectric properties of isoniazid single crystal

S. Dinagaran [a], J. Gajendiran [b,*], S. Gokul Raj [c,*], S. Gnanam [d]

[a] Department of Physics, University College of Engineering Thirukkuvalai, Thirukkuvalai 610 204, Tamil Nadu, India
[b] Department of Physics, Vel Tech Rangarajan Dr.Sagunthala R&D Institute of Science and Technology, Avadi, Chennai 600 062, India
[c] Department of Physics, C.Kandaswami Naidu College for Men, Annanagar, Chennai, 600 102 Tamil Nadu, India
[d] Department of Physics, School of Basic Sciences, Vels Institute of Science, Technology & Advanced Studies (VISTAS), Pallavaram, Chennai 600 117, India

ARTICLE INFO

Keywords:
Single crystal
Slow evaporation
Structural
Optical properties
Dielectric

ABSTRACT

In this study, isoniazid single crystals were synthesized using solvent mediated followed by slow solvent evaporation techniques for testing the electro-optics application. Powder XRD analysis was used to record several scattering peaks for the obtained grown material, and the presence of scattering peak positions results correlated to the reported scattering peak position of the above title compound's orthorhombic crystal structure. Further, the single crystal XRD analysis confirmed the orthorhombic crystal system based on the obtained lattice parameters of synthesized crystal. The grown crystal was scanned using an FT-IR analysis, and its chemically attached functional groups were detected in the spectrum. According to UV–visible studies, isoniazid has a transmittance value of more than 90 %. In addition, the transmittance behavior of the grown compound changed significantly depending on its wavelength. The nonlinear optical property study of the grown crystal was characterized, and the results of the second harmonic generation efficiency values correlate with those of standard reference crystal. Thermal stability and melting temperature of the grown crystal were investigated using TG/DTA studies. The temperature vs weight loss plot revealed weight loss in the temperature range of 225 °C to 400 °C for the grown crystal. Using differential thermo gravimetric analysis (DTA), the melting temperature of the synthesized crystal was determined to be 170 °C. The dielectric constant and dielectric loss responses of grown isoniazid crystals are found to be less at high frequencies and increase exponentially at low frequencies due to the presence of polarization effects.

1. Introduction

Many researchers have focused in recent years on the various types of single crystal developed using different techniques for investigating the suitability of multifunctional based devices like non-linear optical and electro-optics modulation based devices; frequency shifting, optical switching, photonic devices, laser frequency conversion devices, and optical data storage, among others [1–7]. The above-mentioned multifunctional devices necessitate high optical transparency, good transmittance in the visible region, a larger optical band gap value, and good dielectric constant and dielectric loss characteristics. Further, developing such non-linear optical (NLO) activity and electro-optical characteristics in a single crystal is a difficult task in research laboratory. Isoniazid crystals and derivate compounds have been grown using different techniques, and the grown crystals have been analyzed by various instrumentation methods [8–10]. Few researchers have investigated the structural, vibrational and density functional theory (DFT) studies of isoniazid crystals and derivatives compound [1,8–10]. In addition, the aforementioned isoniazid compounds have been tested in biomedical applications, specifically as antitubercular drugs in tuberculosis disease [8].

The aim of this work is to synthesize isoniazid single crystals using solvent-mediated followed by slow solvent evaporation techniques, and then subject the grown crystal to NLO and dielectric applications.

2. Experimental

The flow chart in Fig. 1 depicts the growing step of isoniazid crystals.

Various concentrations (15, 18, 21, 24, and 27 g) of isoniazid salt were dispersed in 100 mL of distilled water at various temperatures

* Corresponding authors.
E-mail addresses: gaja.nanotech@gmail.com (J. Gajendiran), sgokulraj@gmail.com (S. Gokul Raj).

https://doi.org/10.1016/j.optlastec.2022.108576
Received 10 May 2022; Received in revised form 1 July 2022; Accepted 6 August 2022
Available online 13 August 2022

(25 °C to 55 °C) while stirring, and the solubility results are displayed in Fig. 2. The solubility plots clearly show that as the temperature increased from 27.5 °C to 52.5 °C, a higher concentration of isoniazid salt was dissolved, and as a result, the salt gradually became soluble in water. Finally, a saturated solution was obtained. This was due to the thermal treatment causing aqueous dissociation. Based on the above findings, it is possible to identify the solubility and saturation solution of isoniazid salt. The prepared saturated solution was filtered and optimally closed to control evaporation while maintaining a temperature of 30° C. After 20 days, transparent crystals were formed. Fig. 3 depicts a photograph of a grown isoniazid crystal. Table.1 shows the detailed characterizations used in the current work for the synthesized single crystal.

3. Results and discussion

The powder XRD analysis was used to record the diffraction angles of the grown isoniazid crystal from 10° to 60°, as shown in Fig. 4. When the diffraction angle position and corresponding diffraction peaks of the grown crystals were compared to the reported work [11–13], it was confirmed that the grown crystal was the formation of the isoniazid compound. The grown isoniazid compound's X-ray diffraction peaks and corresponding diffraction planes were indexed (CCDC No: 847197). The sharp and intense XRD peaks confirmed the material's crystalline nature.

In addition, a single crystal XRD analysis was performed on the grown material, and the obtained lattice parameter values were compared with Bhat et al. [14] reported lattice parameter values of isoniazid material and its results consolidated as shown in Table.2. Based on the lattice parameter values from Table.2, the grown crystal belongs to an orthorhombic crystal system, which is compared to the reported values of isoniazid crystal.

The molecular vibration modes of a grown crystal were recorded using Fourier Transform Infrared (FT-IR), and its vibration modes were identified and confirmed as isoniazid. Fig. 5 depicts FT-IR spectrum of the isoniazid compound's. Table.3 shows the observed bands as well as their vibrational assignments. Table.3 compares the observed bands to the reported vibrational band values for the respective modes, confirming that the synthesized material is isoniazid.

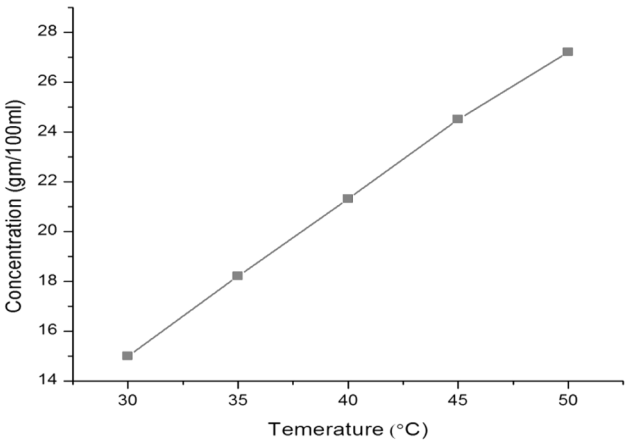

Fig. 2. Solubility curve of isoniazid crystal.

The second harmonic generation (SHG) was confirmed by the observed emission of green light from the Kurtz powder method [15]. At an input power of 1.12 mJ/pulse, the SHG value of synthesized isoniazid was found to be 25 mV. Table.4 compares the experimentally found SHG signal output of the synthesized isoniazid material to that of the standard reference crystal SHG value. The inherent charge exchange tendency over the donor–acceptor bridge network and the moderate dipole moment of isoniazid are the primary factors that contributed to the increase in SHG efficiency of isoniazid crystal over potassium dihydrogen phosphate (KDP). However, the SHG efficiency of isoniazid crystal was found to be lower than that of urea crystal [3].

UV analysis was performed on a 1 mm thick as-grown isoniazid crystal. The transmittance vs wavelength plot, shown in Fig. 6, is characterized in the wavelength range of 200 to 800 nm to examine the

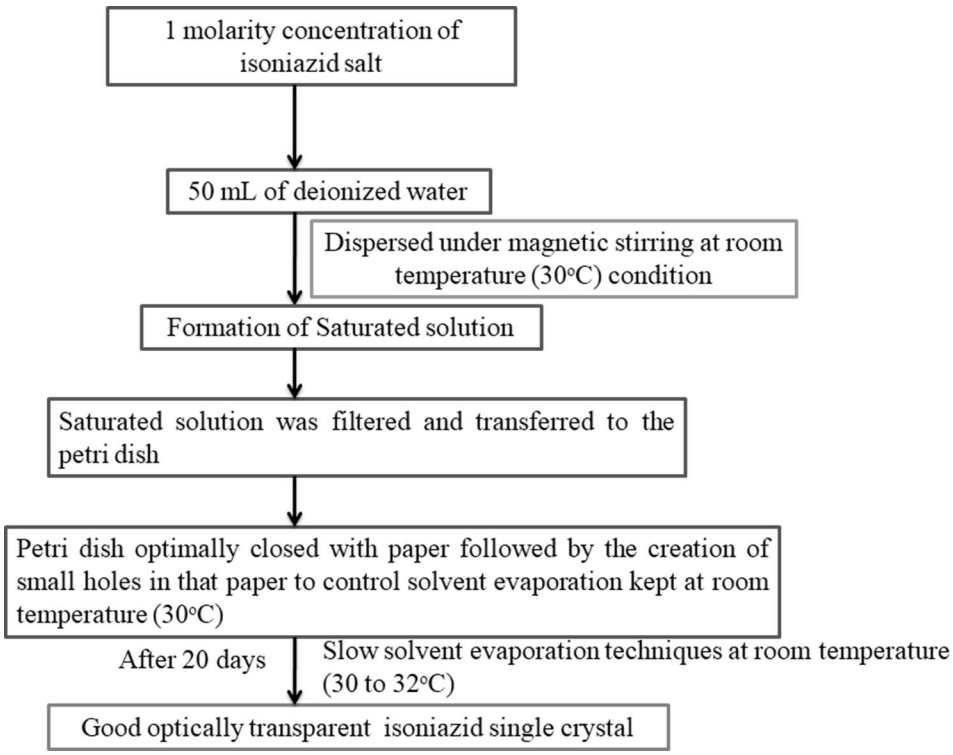

Fig. 1. Isoniazid single crystal growing process.

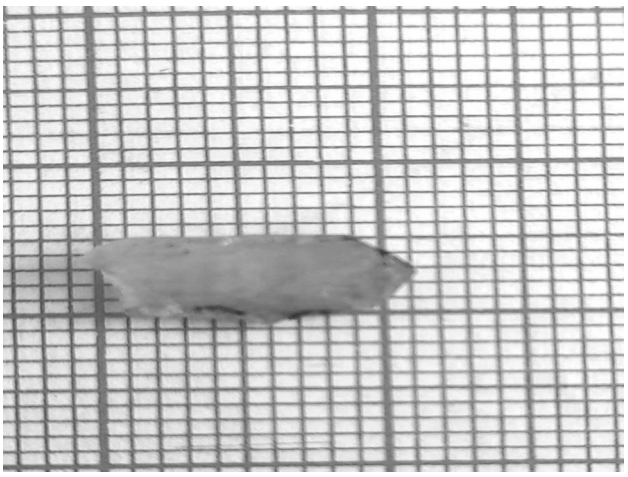

Fig. 3. As-grown isoniazid crystal.

Table 1
Details on the characterization of as-grown isoniazid crystal.

Characterizations	Analytical Instruments details	Specifications
Single crystal XRD	Enraf-Nonius CAD-4 diffractometer	MoK_α radiation λ-0.71073 Å. Data Collection - ω/2θ scan mode.
Powder XRD	Rigaku mini Flex II X-ray diffractometer	CuK_α (λ = 1.54059 Å) radiation, the diffraction pattern was scanned between ranges of 10 to 60°
FT-IR	Perkin-Elmer spectrometer	Wavenumber in the range 400–4000 cm^{-1} by KBr pellet method
Kurtz and Perry powder technique	Indigenously built NLO tester with prolab 170 Nd: YAG laser	Wavelength of 1064 nm with a gaussion pulse width 10 ns with repetition rate of 10 Hz was used
Optical transmission spectrum	Perkin Elmer Lambda 35 UV–vis spectrophotometer	Wavelength recorded in the range 200–1200 nm
TGA/DTA	NETZSCH STA 449F3 simultaneous analyzer	Nitrogen atmosphere at heating rate of 20 °C per minute from 30 °C to 400 °C
Dielectric studies	Keithley 3330 - LCZ meter	Frequency range 1 kHz–40 MHz with a signal strength of $1V_{rms}$

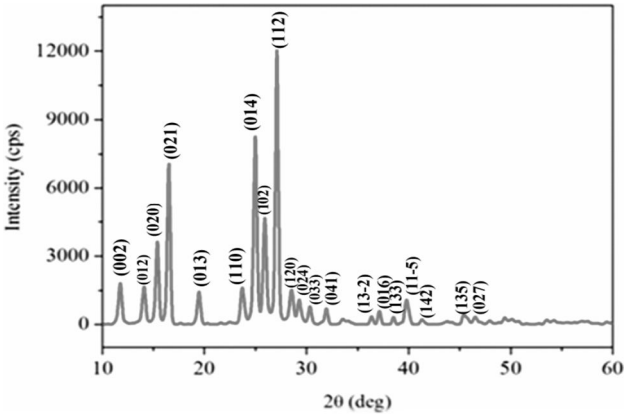

Fig. 4. Powder XRD pattern of isoniazid crystal.

quality of synthesized isoniazid crystal transparency. This optical measurement reveals that the crystal is transparent more than 90 % in the visible wavelength range of 380–800 nm. UV transmittance increases as

Table 2
Lattice parameters of isoniazid crystal.

Lattice parameters	Bhat et al. [14]	In this present work
a	14.915 Å	14.803 Å
b	11.400 Å	11.375 Å
c	3.835 Å	3.854 Å
α	90°	90°
β	90°	90°
ɣ	90°	90°
V	652.06 $Å^3$	648.9 $Å^3$

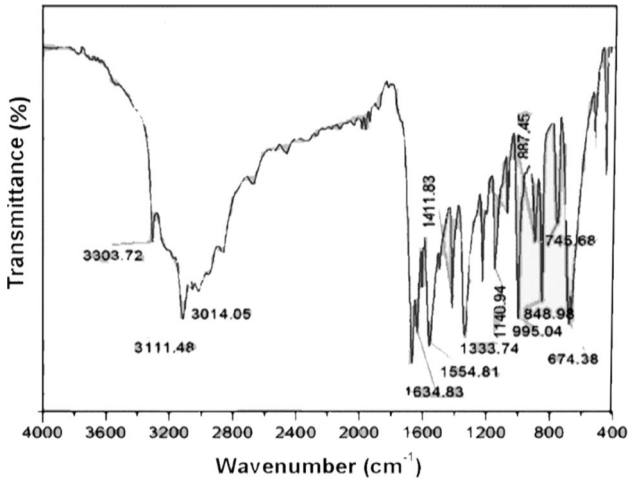

Fig. 5. FT-IR spectrum of isoniazid crystal.

Table 3
FT-IR vibrational band assignments of isoniazid crystal [1,12,13].

Wave number (cm^{-1})	Vibration Assignments
3303	NH stretching
3111	CH Asymmetric stretching
3014	C—H stretching
1634	H_2O
1554	C═N stretching
1333	C—N stretching
1140	NH_3 rocking
848, 995	CH stretching
745	C—C—C Asymmetric bending
674	C—C—C Symmetric bending

Table 4
Comparison of SHG signal output.

Input power mJ/pulse	KDP (mV)	Urea (mV)	Isoniazid crystal (mV)
1.12	14	70	25

the wavelength increases, up to 394 nm. This type of crystal would be used in NLO applications due to its optical transmission range in the visible region. Furthermore, improved optical transmittance in the obtained crystal could be due to factors such as material light absorption of the grown crystal, improved photochemical stability, lower concentration of impurities centres, and the absence of intermediate photon absorbing transition electronic states [3,16–18].

As shown in Fig. 7, the goal of investigating the thermal (TG-DTA, DSC) analysis for isoniazid crystal is to determine thermal stability. According to the TGA curve (Fig. 7a), the isoniazid compound is thermally stable up to 225 °C (green arrow mentioned in Fig. 7a). Following that, in the temperature range of 225 °C to 400 °C, the weight loss was found to be 92 %. The resulting DTA trace revealed a sharp endotherm

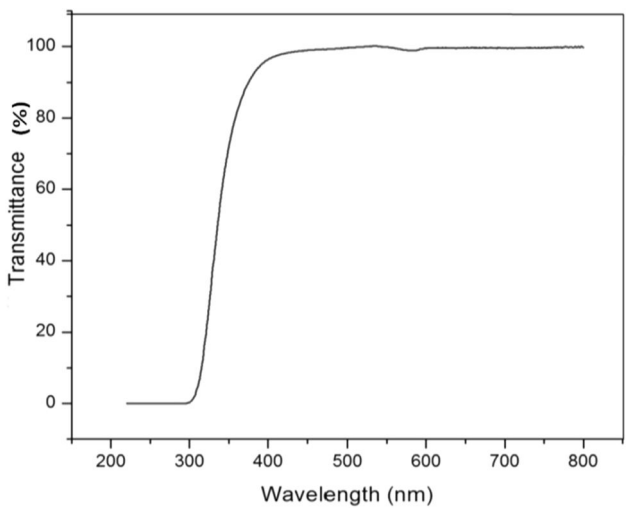

Fig. 6. UV–vis transmittance spectrum of isoniazid crystal.

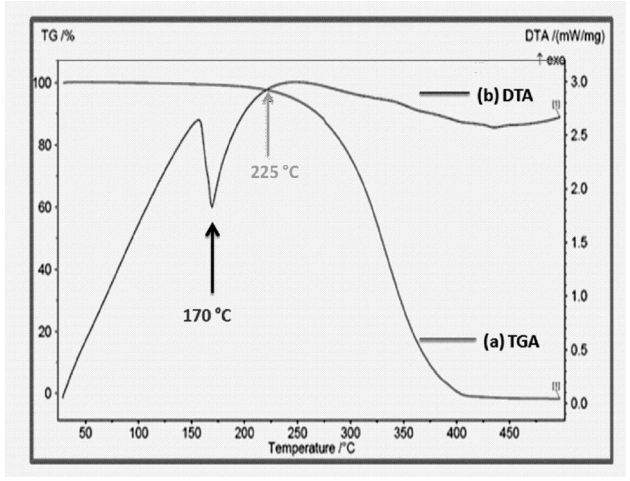

Fig. 7. (a) TGA and (b) DTA curve of isoniazid crystal.

peak at 170 °C (blue arrow in Fig. 7b). It refers to isoniazid's melting point [11].

The dielectric constant vs logarithmic frequency plot at all temperatures (Fig. 8a) revealed that higher dielectric constant values were detected at lower frequencies up to 2 Hz, but dielectric constant values gradually decreased as the frequency level increased. Further, as the frequency level increases from 2 Hz to 7 Hz, dielectric constants appear in a steady state [19]. The presence of electronic, ionic, space charge and orientational polarization may cause a high dielectric constant at lower frequency levels because many electric dipoles are aligned in a particular direction [19]. When the synthesized crystal was applied at a higher frequency, a constant movement of dielectric constant values was observed, which could be attributed to the only contribution of the space charge polarization effect and the absence of the remaining polarization effect. The inability to align the dipole moment in a specific direction is another cause of constant dielectric loss movement. Furthermore, dielectric loss behaviour changes were observed at the applied frequency level from low to higher regions at various temperatures (313 K and 343 K) due to the presence or absence of the above polarization effect using confirmed logf vs dielectric loss plots (Fig. 8b).

Because of the lower dielectric constant of the as-grown crystal, lower polarizability occurred, resulting in low power consumption and decreased RC delay, as well as an increase in the material's SHG efficiency. In addition, the lower dielectric loss of isoniazid crystal reveals its high optical quality and low active imperfections [20–23]. Isoniazid crystal's lower dielectric properties imply that it is used for SHG and photonic-based devices.

4. Conclusion

A single crystal of isoniazid material was successfully grown using the slow evaporation technique. Various concentrations of isoniazid salt were dispersed in distilled water under magnetic stirring at different temperatures, and the saturation solution of isoniazid salt was determined using a solubility test. The observed strong diffraction peaks from the as-grown crystal's XRD pattern and lattice constant, which are closely matched with the reported XRD pattern and unit cell parameters of the isoniazid compound. Single crystal XRD measurements also confirmed that the crystal is an orthorhombic system. In the synthesized crystal, the FT-IR was used to identify the chemically attached various vibrational bands and their corresponding functional groups. Optical transmittance spectrum studies show that the crystal's transparency is in the 395–800 nm range, indicating that it has the potential to be used in opto-electronic devices. According to TGA results, the isoniazid compound is thermally stable up to 225 °C. DTA analysis was used to determine the melting point of isoniazid at 170 °C. The SHG test revealed that as-grown isoniazid crystals outperform the standard reference crystal KDP. The dielectric studies revealed that the isoniazid crystal has a lower dielectric constant and dielectric loss, indicating that the good optical quality and fewer active imperfections and their consequences would be suitable for SHG and photonic-based devices.

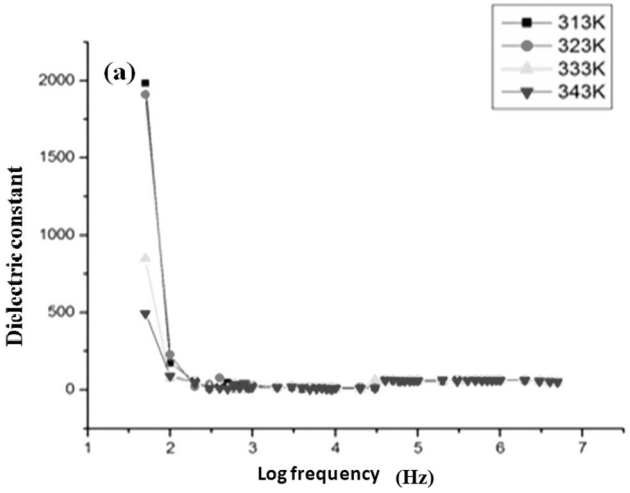

Fig. 8a. Dielectric constant vs Log f plot of as-grown isoniazid crystal.

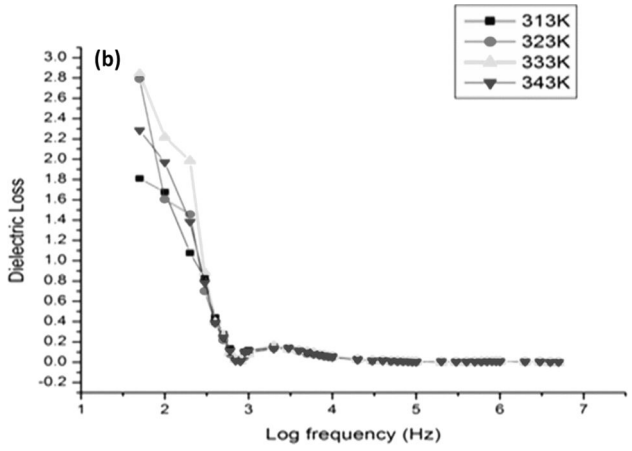

Fig. 8b. Dielectric loss vs Log f plot of as-grown isoniazid crystal.

CRediT authorship contribution statement

S. Dinagaran: Methodology, Investigation, Writing – original draft. **J. Gajendiran:** Investigation, Writing – original draft, Writing – review & editing, Conceptualization. **S. Gokul Raj:** Investigation, Writing – original draft, Writing – review & editing. **S. Gnanam:** Investigation, Writing – original draft, Writing – review & editing.

Declaration of Competing Interest

The authors declare that they have no known competing financial interests or personal relationships that could have appeared to influence the work reported in this paper.

Data availability

Data will be made available on request.

References

[1] M. Buvaneswari, R. Santhakumari, C. Usha, R. Jayasreec, Suresh Sagadevan, analysis and thermodynamic properties of vanillin isonicotinic hydrazide single crystal Synthesis, growth, structural, spectroscopic, optical, thermal, DFT, HOMO-LUMO, MEP, NBO, J. Mol. Struct. 1243 (2021), 130856.

[2] Rylan J. Terry, Daniel Vinton, Colin D. McMillen, Xiang fengChen, Lin Zhu, Joseph W. Kolis, Hydrothermal single crystal growth and structural investigation of the stuffed tridymite family as NLO materials, J. Alloys Compd. 909 (2022).

[3] Mohd Anis, M.S. Pandian, M.I. Baig, P. Ramasamy, G.G. Muley, Monocrystal growth and characterization study of α- and γ-polymorph of glycine to explore superior performance of γ-glycine crystal, Mater. Res. Innov. 22 (2018) 409–414.

[4] M.I. Baig, Mohd Anis, G.G. Muley, Influence of tartaric acid on linear-nonlinear optical and electrical properties of KH_2PO_4 crystal, Optic. Mater. 72 (2017) 1–7.

[5] Mohd Anis, G. G. Muley, M. I. Baig, Waseem Ahmed Khan, S. P. Ramteke, Ehab El Sayed Massoud, Optimizing first-, second- and third-order optical traits of zinc tris-thiourea sulphate (ZTS) crystal by L-tyrosine for photonic device applications, Indian J. Phy (2022) Article in Press.

[6] S.P. Ramteke, G.G. Muley, M.I. Baig, A. Ibrahim, M. Aslam, Manthrammel, Mohd Shkir, Mohd Anis, , Optimizing growth, linear and 3rd order nonlinear optical traits of potassium aluminium sulfate (KAS) crystal by tuning pH for photonic device applications, Inorg. Chem. Commun. 140 (2022), 109484.

[7] M.I. Baig, S.S. Hussaini, H. Elhosiny Ali, M. Anis, Analyzing $_L$-valine effect on structural, mechanical, optical and electrical traits of bis-thiourea cadmium chloride (BTCC) crystal, J. Mater. Sci: Mater. Electron. 33 (2022) 8218–8225.

[8] EbruKoçak Aslan, V. SivaKrishna, S.J. Armaković, StevanArmaković, OnurŞahin, ToneTønjum, Miyase GözdeGündüz, Linking azoles to isoniazid via hydrazone bridge: Synthesis, crystal structure determination, antitubercular evaluation and computational studies, J. Mol. Liq. 354 (2022), 118873.

[9] M. Cocu, I. Bulhac, E. Coropceanu, E. Melnic, S. Shova, O. Ciobanica, V. Gutium, P. Bourosh, SergiuShova, Olga Ciobanica, VictoriaGutium, Paulina Bourosh, Synthesis and structure of new mononuclear octahedral cobalt(III) dioximates derived from isonicotinic hydrazide, J. Mol. Struct. 1063 (2014) 274–282.

[10] M. Pocrnic, D. Kontrec, SnežanaMiljanic, Zeljka Soldin, Ana Budimir, Nives Galic, Gallium(III) complexes of aroylhydrazones derived from nicotinic acid hydrazide in solid state and in solution, J. Mol. Struct. 1227 (2021), 129564.

[11] Jean Baptiste Ngilirabanga, Marique Aucamp, Paulo Pires Rosa, Halima Samsodien1, Mechanochemical Synthesis and Physicochemical Characterization of Isoniazid and Pyrazinamide Co-crystals with Glutaric Acid, Front Chem. 8 (2020), 595908.

[12] B. Saifullah, P. Arulselvan, M.E.E. Zowalaty, S. Fakurazi, Thomas J Webster, Benjamin M Geilich, Mohd Zobir Hussein, Development of a biocompatible nanodelivery system for tuberculosis drugs based on isoniazid-Mg/Al layered double hydroxide, Int. J. Nanomed. 9 (2014) 4749–4762.

[13] F. Afinjuomo, T.G. Barclay, A. Parikh, R. Chung, Y. Song, G. Nagalingam, J. Triccas, L. Wang, L. Liu, J.D. Hayball, N. Petrovsky, S. Garg, Synthesis and Characterization of pH-Sensitive Inulin Conjugate of Isoniazid for Monocyte-Targeted Delivery, Pharmaceutics 11 (2019) 555.

[14] T.N. Bhat, T.P. Singh, M. Vijayan, Isonicotonic Acid Hydrazide - a Reinvestigation, Acta Cryst. B 30 (1974) 2921–2922.

[15] P. Lalitha, A. Sinthiya, Sugumari Vallinayagam, Kaushik Pal, Growth dynamics and spectroscopic characterization strategies of 'L-proline' doped potassium hydrogen phthalate single crystal structural avenue, J. Mol. Struct. 1249 (2022), 131647.

[16] M.I. Baig, M.D. Mohd Anis, A.M. Shirsat, H.H. Alshehri, S.S.H. Somaily, Exploring impact of Zn^{2+} on laser induced optical and electrical traits of KH_2PO_4 crystal for NLO device applications, Optik. 227 (2021), 165998.

[17] M. Anis, S.S. Hussaini, M.I. Baig, M.I. Anis, E.E.S. Massoud, Ehab El Sayed Massoud, Investigating optical, electrical, and mechanical traits of thiourea admixtured KDP single crystals to explore NLO device applications, J. Mater. Sci: Mater. Electron. 32 (18) (2021) 23206–23214.

[18] M.I. Baig, Mohd Anis, M.D. Shirsat, H.H. Somaily, S.S. Hussaini, Exploring linear-nonlinear optical, dielectric and microscopic traits of sulphamic acid crystal exploiting Zn^{2+} for photonic device applications, J. Mater.Sci: Mater. Electron. 32 (2021) 16445–16455.

[19] L.R. Keerthi, S. Anand, S. Kalainathan, D. Jaikumar, Investigation on the growth, optical, electrical, thermal and third order NLO properties of 2-(4-methlybenzylidene) malononitrile (MBM) single crystal, Optic. Mater. 109 (2020), 110216.

[20] M.I. Baig, M.D. Mohd Anis, S.S. Shirsat, H.A. Hussaini, Comparative analysis of pristine and Cd^{2+} influenced potassium acid phthalate single crystal for photonic device applications, Optik. 203 (2020), 163903.

[21] M.I. Mohd Anis, A.M. Baig, H.H.S. Alshehri, Experimental analysis of pure and L tyrosine influenced bis-thiourea zinc acetate (BTZA) crystal for NLO device applications, Optik. 220 (2020), 165100.

[22] M. Anis, S. Mohd Shkir, M.I. AlFaify, A.M. Baig, H.A. Alshehri, Exploring remarkable impact of thiourea in enhancing the performance of $NH_4H_2PO_4$ single crystal for photonic device applications, Mater. Chem. Phy. 246 (2020), 122809.

[23] M. Saravanakumar, J. Chandrasekaran, M. Krishnakumar, B. Babu, G. Vinitha, Mohd Anis, Experimental and quantum chemical studies on SHG, Z-scan and optical limiting investigation of 2-amino-5-bromopyridinium trifluoroacetate single crystal for optoelectronic applications, J. Phy. Chem. Solids. 136 (2020), 109133.